JTTEE5 15:708-716
DOI: 10.1361/105996306X147027
1059-9630/$19.00 © ASM International

Peer Reviewed

Photographing Impact of Plasma-Sprayed Particles on Metal Substrates

André McDonald, Mario Lamontagne, Sanjeev Chandra, and Christian Moreau

(Submitted March 1, 2006; in revised form March 27, 2006)

Plasma-sprayed, molten molybdenum particles (~40 μm diameter) were photographed during impact (with velocity ~110 m/s) on Inconel surfaces that were maintained at either room temperature or at 400 °C. Some samples were also preheated at 400 °C for 3 h and then air-cooled to room temperature before spraying. A droplet approaching the surface was sensed using a photodetector, and after a known delay, a fast charge-coupled device camera was triggered to capture images of the spreading splat from the substrate front surface. A rapid two-color pyrometer was used to collect the thermal radiation from the impacting particles to follow the evolution of their temperature and size after impact. Molten molybdenum particles impacting the surfaces at room temperature disintegrated and splashed after achieving a maximum diameter >400 μm. Impact on preheated and heated Inconel produced splats with maximum diameters between 200 and 300 μm with less fragmentation. The cooling rate of splats on preheated Inconel was larger than that of splats on nonheated Inconel. Surface analysis showed that preheating Inconel reduced the surface skewness and kurtosis, resulting in improved splat-substrate contact.

Keywords cooling rate, kurtosis, roughness, skewness, surface oxidation, two-color pyrometry

1. Introduction

Studies have shown that the temperature and surface conditions of the substrate on which plasma-sprayed particles impact influence the extent of splashing and splat morphology (Ref 1-6). Application of an organic layer to stainless steel substrates was found to induce splashing of plasma-sprayed nickel (Ref 6). Preheating the substrates to a temperature above the boiling point of the organic compound reduced splat splashing. The effect of substrate preheating has received considerable attention in recent years. A short-duration pulse laser was used to preheat polished Ti-6Al-4V substrates before spraying (Ref 4) to remove adsorbates/condensates. It was found that increasing the substrate temperature reduced the occurrence of fragmentation and produced disk-like splats (Ref 4). It has been speculated that disk-like splats on preheated surfaces are formed due to good contact between the substrate and the splat (Ref 1, 7). Improved splat-substrate contact increases the solidification rate of the splat and reduces splashing (Ref 1). Measurements of the cooling rate of molybdenum splats on heated glass were an order of magnitude larger than those on nonheated glass (Ref 2, 8).

This article was originally published in *Building on 100 Years of Success, Proceedings of the 2006 International Thermal Spray Conference* (Seattle, WA), May 15-18, 2006, B.R. Marple, M.M. Hyland, Y.-Ch. Lau, R.S. Lima, and J. Voyer, Ed., ASM International, Materials Park, OH, 2006.

André McDonald and **Sanjeev Chandra,** Center for Advanced Coatings Technology, Department of Mechanical and Industrial Engineering, University of Toronto, Toronto, ON, M5S 1A4, Canada; and **Mario Lamontagne** and **Christian Moreau,** National Research Council, Canada Industrial Materials Institute, Boucherville, QC, J4B 6Y4, Canada. Contact e-mail: mcdonald@mie.utoronto.ca.

Prolonged heating of metal substrate surfaces was reported to increase splat splashing and reduce adhesion (Ref 5, 9). Pech et al. (Ref 5) have shown that short-term heating of metallic substrates improves coating adhesion, while prolonged heating reduces it. The change was attributed to the growth of thick oxide layers on the surface. Nickel coatings deposited on stainless steel coupons maintained at 650 °C had larger adhesion strengths than those on coupons that were cooled before spraying (Ref 9). It was proposed that the removal of the surface moisture permitted a better penetration of surface cavities, improving splat contact and adhesion (Ref 9). It was also speculated that the surface oxidation contributed partially to the increase in splat contact and coating adhesion strength.

The surface topology of the oxidized surfaces has been found to influence significantly the flattening and solidification of plasma-sprayed particles (Ref 10). In this study, the surface topology has been characterized by using three roughness parameters: average roughness (R_a); skewness (R_{sk}); and kurtosis (R_{ku}) (Ref 10). The R_{sk} characterizes the symmetry of the rough surface profile (Ref 11), while R_{ku} shows the degree of pointedness of the asperities on the surface (Ref 11). It was found that preheating the substrate increased the R_a only slightly but changed the R_{sk} significantly. On the preheated AISI 304 stainless steel substrates, the R_{sk} was negative, and disk-like splats were observed. On nonheated surfaces, where the R_{sk} was positive, splat splashing occurred (Ref 10). Further experimental work is needed to understand how substrate heating changes the contact between the splat and the substrate, and how this affects splat adhesion and cooling.

Several articles have been published that have described methods of measuring the splat cooling rate (Ref 12-14), and of photographing the splats during and after spreading (Ref 3). Two-color pyrometry and photographs of the splat have been used to obtain the splat size, temperature evolution, and cooling rate. The temperature evolution obtained from two-color pyrometry was used to show that the cooling rate of nickel on a pre-

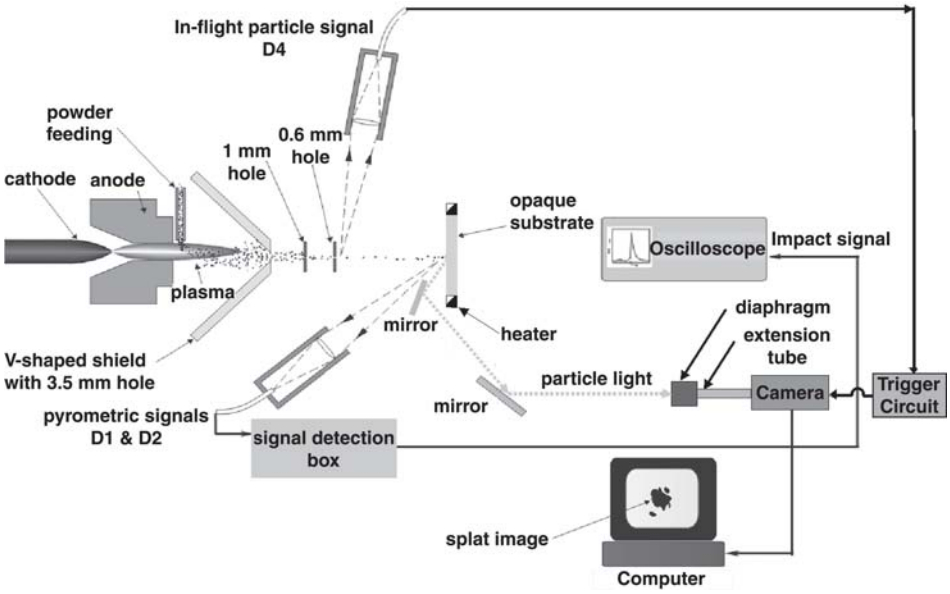

Fig. 1 Schematic of the experimental assembly

heated stainless steel substrate is almost an order of magnitude larger than that on nonheated stainless steel (Ref 12). Other investigators have used two-color pyrometry to conduct temperature measurements (Ref 13, 14). Recently, Shinoda et al. (Ref 13) used this technique in an in situ measurement system to monitor the thermal evolution of plasma-sprayed zirconia particles that impinged on quartz glass substrates. Mehdizadeh et al. (Ref 3) have used a nanosecond duration laser coupled with a charge-coupled device (CCD) camera to capture images of the splat during spreading, while simultaneously measuring the temperature. Photographing the splat, while measuring the temperature, provides useful information to better understand how prolonged substrate heating affects splat adhesion and cooling.

The objectives of this study were: to photograph molybdenum particles that impacted coupons of Inconel preheated, and maintained at room temperature and at 400 °C; to use two-color pyrometry to measure the temperature evolution and cooling rates of the splats on these surfaces; and to use roughness parameters to explain the increased cooling rate and smaller diameters of the splats on preheated Inconel.

2. Experimental Method

A schematic diagram of the experimental setup is shown in Fig. 1. An SG100 plasma torch (Praxair Surface Technologies, Indianapolis, IN) was used to melt and accelerate molybdenum powder particles (SD152; Osram Sylvania Chemical and Metallurgical Products, Towanda, PA), sieved to −63 + 38 μm. The powder feed rate was <1 g/min. The substrates were mirror-polished Inconel 625 (hereafter referred to as "Inconel" in this article) (High Temp Metals, Sylmar, CA) and glass slides (Fisher Scientific, Pittsburgh, PA) that were washed with water and ethanol, and were dried in an oven at 140 °C for 30 min. The backs of the glass slides were painted black to provide a contrasting background when splat images were captured. To heat the substrate during spraying, the samples were placed in a copper substrate holder that included heater cartridge wires (Omega, Laval, QC, Canada). Some Inconel and glass samples were heated in air for 3 h at 400 °C and were allowed to cool to room temperature (these substrates are referred to as "preheated" in this study).

The plasma torch was operated with a voltage of 35 V and a current of 700 A. The plasma gas mixture was argon, at a flow rate of 50 L/min (LPM), and helium, at a flow rate of 24.5 LPM. The torch was passed rapidly across the substrates. To protect the substrate from an excess of particles and heat, a V-shaped shield was placed in front of the torch. This V-shaped shield had a 3.5 mm hole through which particles could pass. To reduce the number of particles landing on the substrate, two additional barriers were placed in front of the substrate, the first of which had a 1 mm hole, and the second a 0.6 mm hole. All of the holes were aligned to permit passage of the particles with a horizontal trajectory (Fig. 1).

After exiting the third barrier and just before impacting the substrate, the thermal radiation of the particles was measured with a two-color pyrometric system (D_1 and D_2 sensor). Mehdizadeh et al. (Ref 3) have described this system in detail. The system included an optical sensor head that consisted of a custom-made lens with a 0.21 magnification, which focused the collected radiation onto an optical fiber with an 800 μm core (Ref 3). This optical fiber was covered with an optical mask that was opaque to near-infrared radiation, except for three slits. Two of the slits, with dimensions of 30 × 150 μm and 30 × 300 μm, were used to detect the thermal radiation of the in-flight particles. The radiation was used to calculate the temperature and velocity of the in-flight particles (Ref 3, 15). The largest slit, measuring 150 × 300 μm, was used to collect the thermal radiation of the particle as it impacted and spread on the substrate. With the thermal radiation from this slit, the splat temperature, diameter, and

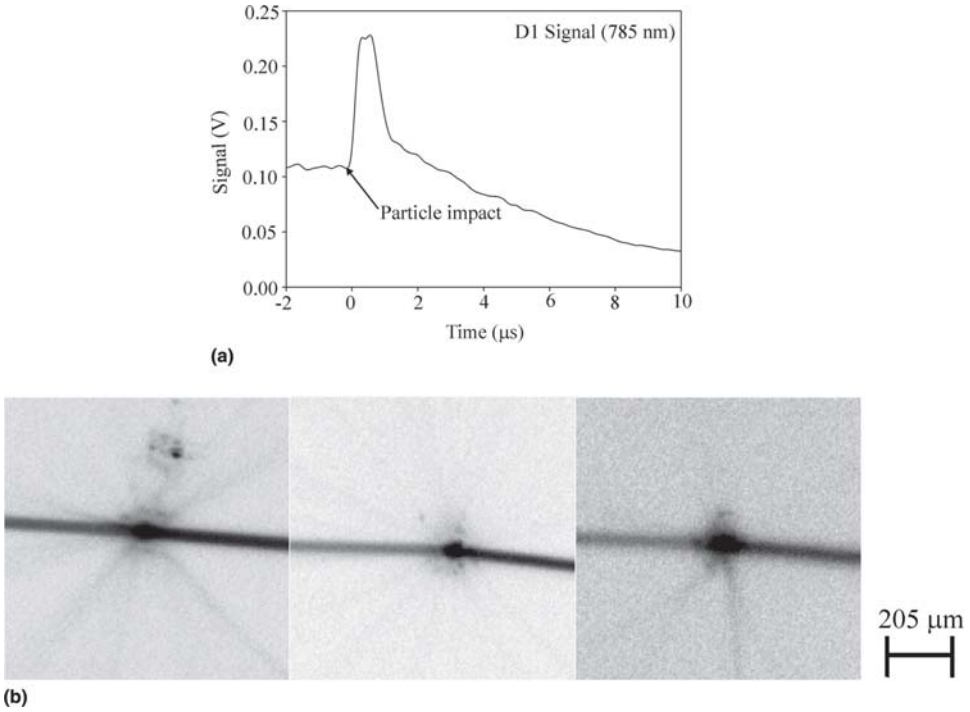

Fig. 2 (a) A typical thermal emission signal and (b) images of molybdenum splats on Inconel held at 400 °C

cooling rate were calculated at 200 ns intervals after the impact. The average in-flight velocity of the droplet was calculated by dividing the known distance between the centers of the two smaller slits by the measured time of flight. The distance between the centers of the two small slits was approximately 65 μm.

The collected thermal radiation was transmitted through the optical fiber to a detection unit that contained optical filters and two photodetectors. The radiation beam was divided into two equal parts by a beam splitter. Each signal was transmitted through a bandpass filter with a wavelength of either 785 or 995 nm and then detected using a silicon avalanche photodetector (model C30817; RCA, Durant, OK). The photodetector had a response time of <0.1 μs (Ref 16). The ratio of the radiation intensity at these wavelengths (referred to as D_1 and D_2, respectively) was used to calculate the particle temperatures with an accuracy of ±100 °C (Ref 15). The signals were recorded and stored with a digital oscilloscope.

A 12-bit CCD camera (QImaging, Burnaby, BC, Canada) was used to capture images of the spreading particles. The electronic shutter of the camera was triggered to open by a signal from the D_4 sensor (Fig. 1). The camera was attached to a 30 cm long optical extension tube that was connected to a diaphragm (Tominon, Waltham, MA). The diaphragm included a lens with a 135 mm focal length and f-stop from 4.5 to 32. The diaphragm was set to f-stop 16, so that the diameter was 8.4 mm. To photograph the in-flight particles and the splats, the shutter of the camera was opened for about 500 μs, with no added illumination. This produced single, integrated images of the splats at the maximum spread diameter. The images captured by the camera were then digitized by a frame grabber and recorded on a personal computer.

3. Results and Discussion

3.1 Impact and Spreading

Previous studies (Ref 3, 8) have used short-duration laser illumination to study the in situ spreading of molybdenum splats on glass, while others (Ref 2, 12, 16) have used rapid two-color pyrometry to measure the splat cooling rates of molybdenum and yttria-stabilized zirconia. Figures 2, 3, and 4 show typical thermal emission signals from the D_1 (785 nm) sensor and integrated images of different particles on Inconel held at 400 °C, at room temperature, and on preheated samples, respectively. The thermal emission signals were used to calculate the in-flight temperature and velocity of the particle and the maximum spread time of the splat. The maximum spread time is taken as the time required for reaching the maximum voltage on the thermal emission signals. This corresponds closely to the moment the splat reaches its maximum diameter. To emphasize the portion of the signals that is representative of the spreading splat, the two small peaks, which were used to calculate the in-flight velocity and temperature, are not shown in the figures. The average (± standard error of the mean) in-flight temperature of the particles was 2830 ± 25 °C, and the average in-flight velocity was 110 ± 2 m/s (30 samples). The standard error of the mean value, calculated by dividing the SD by the square-root of the number of samples (Ref 17), is shown with each average. In addition to the splats at the maximum extent, the images also show two comet-like streaks. The streak on the right represents the path of the in-flight particle, and the other its reflection in the mirror-polished Inconel. ImageJ imaging software (National Institutes of Health, Bethesda, MD) was used to estimate the maximum diameters from the images by calculating the area A_c and

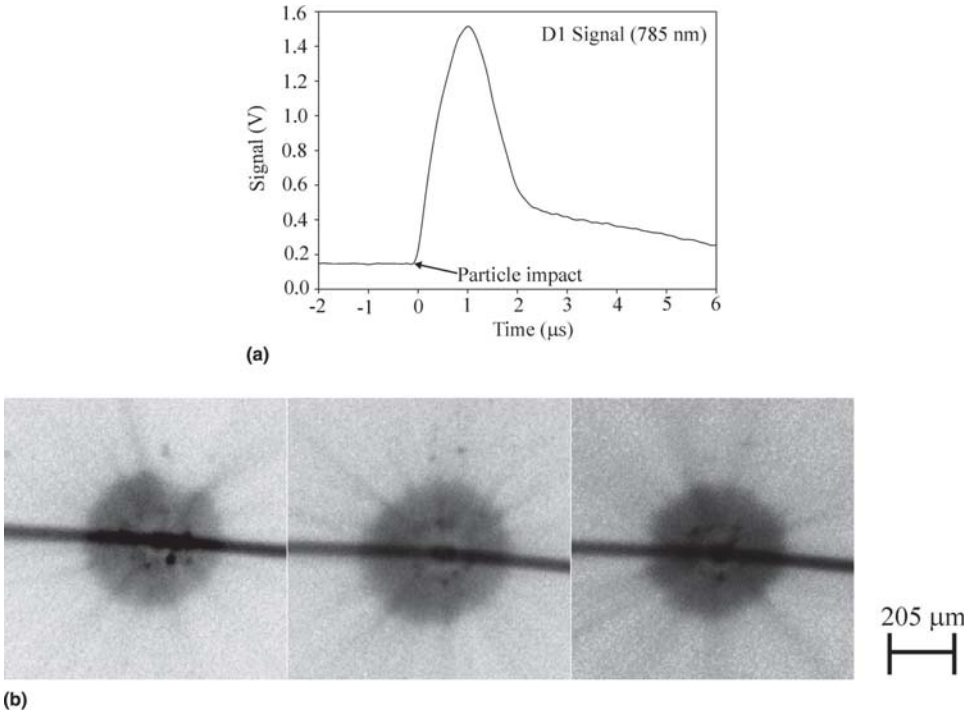

Fig. 3 (a) A typical thermal emission signal and (b) images of molybdenum splats on Inconel held at room temperature

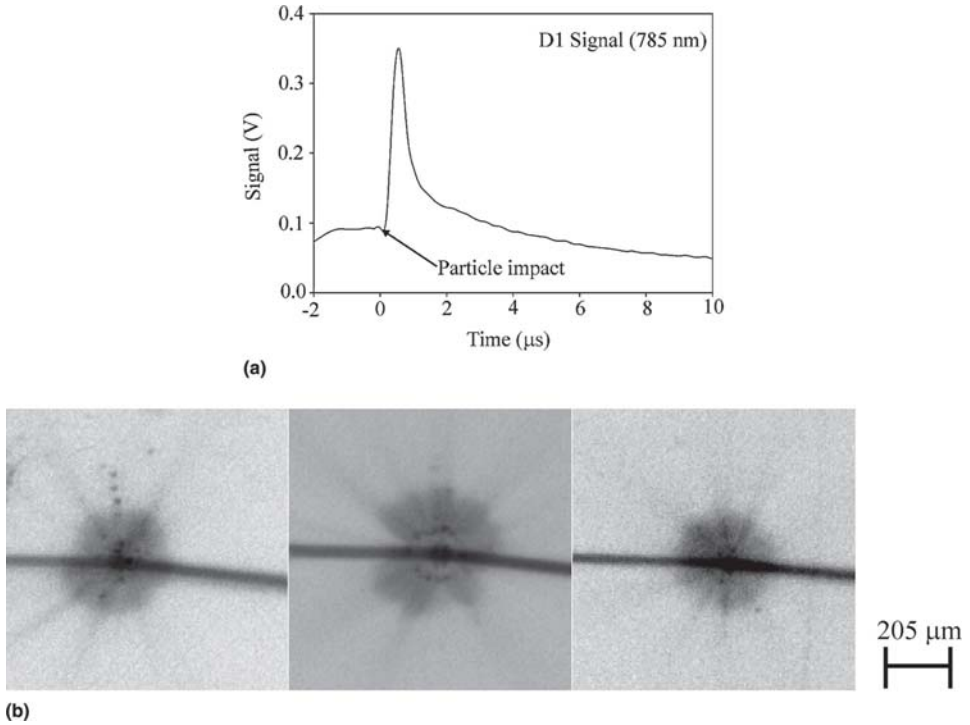

Fig. 4 (a) A typical thermal emission signal and (b) images of molybdenum splats on preheated Inconel

perimeter P of the circular, white splats, and using the hydraulic diameter formula, $D_{max} = 4A_c/P$. In-flight particle diameters were estimated by measuring the width of the comet-like streaks in the images.

On Inconel heated to 400 °C, the particles spread to an average maximum diameter of 165 ± 10 μm (12 samples) (Fig. 2b). On Inconel held at room temperature, the average maximum spread diameter was almost three times larger, at 440 ± 10 μm

(12 samples) (Fig. 3b). The morphology of the splats at the maximum extent on preheated Inconel was similar to that on nonheated Inconel. The maximum spread diameter on this substrate was 320 ± 30 μm (six samples) (Fig. 4b). The thermal emission signals show that the maximum spread times of the splats on Inconel held at room temperature, at 400 °C, and on preheated samples were 0.5, 1.1, and 0.6 μs, respectively (Fig. 2a, 3a, and 4a, respectively).

The thermal emission signals indicate the occurrence of splat material loss. Material loss does not begin until after the liquid film of the splat begins to fragment and material is ejected from the film. It has been shown that on a typical thermal emission signal for the impact of molybdenum on nonheated glass, the transition from a period of relatively high voltage decrease, immediately after achieving the maximum diameter, to a period of slow voltage decrease indicates that material exited the pyrometric field of view (Ref 18).

For impact on nonheated and preheated Inconel, Fig. 3 and 4, respectively, show that the slope of the thermal emission signal changed significantly (~1 to 2 μs) after impact, suggesting material loss. Figure 2, which shows impact on heated Inconel, does not show this change on the thermal emission signal. Scanning electron microscope (SEM) micrographs of the splats, after spreading and solidification (Fig. 5), show that after significant fragmentation and material loss the average final diameter of the splat on the nonheated Inconel was 70 ± 3 μm (Fig. 5a). The final diameter measured was that of the central portion of the splat that remained mostly intact, excluding the ring of debris and long fingers formed due to splashing. Fragmentation was slightly reduced on the preheated Inconel (Fig. 5b). On this surface, the average final diameter was 80 ± 3 μm. Fragmentation and material loss was further reduced on the heated Inconel surface (Fig. 5c), resulting in an average final splat diameter of 100 ± 5 μm. The fragmented, flower-like morphology of the central portion of the splat remaining on the surface (Fig. 5c) has been attributed to substrate melting beneath the splat (Ref 19).

The temperature evolutions, determined from the pyrometric signals, are shown in Fig. 6. The cooling rate of the splat is the slope of the line originating from the temperature when the splat was at the maximum extent. Table 1 shows the average cooling rates and the standard errors of the mean on each surface. Figure 6 and Table 1 show that the cooling rate on Inconel held at 400 °C (3.4×10^8 K/s) was more than three times larger than that on nonheated Inconel (1.2×10^8 K/s), but about two times larger than that on preheated Inconel (2.2×10^8 K/s). The cooling rate was approximately two times larger on the cold, preheated Inconel than on the nonheated Inconel. These differences in the cooling rates suggest that the physical contact between the splat and the Inconel held at 400 °C was improved by heating, increasing the heat transfer. This has been attributed to the absence of adsorbates/condensates on the heated surface (Ref 7, 10). After solidification, the fragmented, flower-like morphology of the splat, due to substrate melting (Ref 19), is more pronounced on the heated Inconel (Fig. 5c). This may be due to the larger cooling rates and improved physical contact between the splat and the surface.

It was observed that when the cooling rate was on the order of 10^8 K/s, the temperature of the liquid molybdenum splat fell below the melting point (2617 °C), a few microseconds after impact (Ref 8). Figure 6 shows that on all the Inconel surfaces,

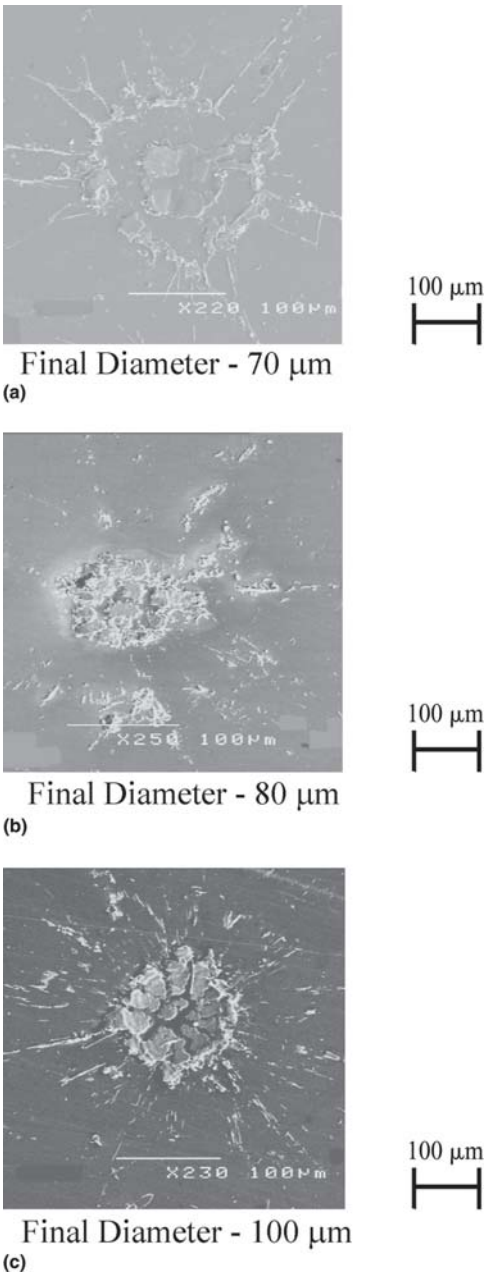

Fig. 5 Images of molybdenum splats after solidification on Inconel (a) at room temperature, (b) preheated, and (c) at 400 °C

the temperature of the liquid splat fell below the melting point, possibly due to undercooling (Ref 8).

Molybdenum particles subjected to approximately the same in-flight parameters were sprayed on glass. It was found that the maximum spread diameter on glass heated to 400 °C was 210 ± 20 μm, and on nonheated glass it was 410 ± 10 μm. The maximum spread times were 0.6 and 1.6 ± 0.1 μs, respectively. These results show that the type of substrate may affect the maximum spread time more than the maximum spread diameter. On nonheated surfaces, the maximum spread time varied by 45%, and the maximum spread diameter by <10%. On the heated surfaces, the maximum spread time was ~15% larger on heated glass than

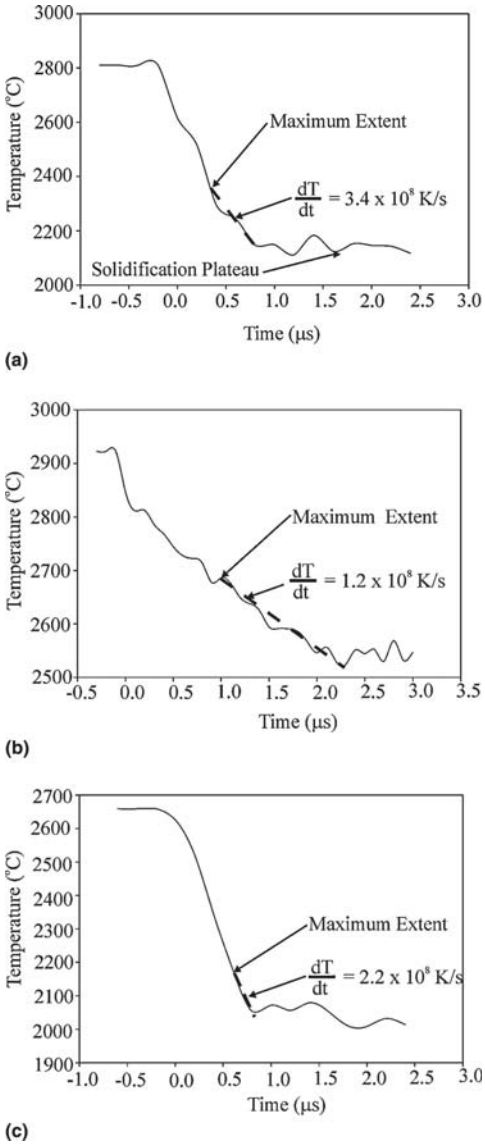

Fig. 6 Typical temperature evolution of molybdenum on Inconel (a) at 400 °C, (b) at room temperature, and (c) preheated

Table 1 Average cooling rates on Inconel substrates

Inconel 625	dT/dt, K/s
Heated (400°C)	$(3.4 \pm 0.4) \times 10^8$
Nonheated	$(1.2 \pm 0.5) \times 10^8$
Preheated	$(2.2 \pm 0.4) \times 10^8$

on heated Inconel, while the maximum spread diameter varied by 20%. Physical contact between the splat and the substrate is improved when the substrate is heated (Ref 1, 7). The smaller difference in the maximum spread times on the heated substrates is probably due to the improved splat-substrate contact and interaction. The cooling rates on glass were lower than those on Inconel. On heated glass, the cooling rate was $(2.1 \pm 0.3) \times 10^8$ K/s, and on nonheated glass it was $(1.1 \pm 0.3) \times 10^8$ K/s. The larger thermal conductivity of Inconel (10 W/m/K), compared with that of glass (3 W/m/K), contributed to the larger cooling rate.

3.2 Surface Topology and Splat-Substrate Contact

Preheating Inconel appears to improve the contact between the splat and the metal substrate because: the average final splat diameter is larger on this surface (80 μm) than on the nonheated surface (70 μm); and the average cooling rate is twice as large. It has been speculated that prolonged heating of metallic substrates promotes the growth of an oxide layer that may affect the spreading dynamics and adhesion of the splat to the substrate (Ref 1, 5, 9). It has been shown that, due to preheating, the oxide layer growth on AISI304 steel induces changes in the surface roughness.

Atomic force microscopy (Veeco Metrology Group, Santa Barbara, CA) was used to determine the roughness and topology of the substrate surface. Figure 7 shows the surface topology of glass and Inconel before and after prolonged preheating at 400 °C. Preheating the Inconel surface greatly increases the number of asperities (Fig. 7a), as the oxide layer becomes thicker. On glass, where preheating does not promote the growth of a new oxide layer, the changes are negligible (Fig. 7b). Three parameters for characterizing the roughness were studied: R_a; R_{sk}; and R_{ku}. The R_a is the arithmetic average of the height of the surface asperities, above a hypothetical, smooth plane. The R_{sk} and R_{ku} may be used to give a more comprehensive description of the surface topology. The R_{sk} shows the degree of symmetry of the rough surface profile and can be used as a measure of the balance between the peaks and valleys of the asperities (Ref 11). The R_{ku} shows the degree of pointedness or bluntness of the asperities on the surface (Ref 11). Smaller R_{sk} values indicate that the surface topology profile has asperities with large plateaus and single deep valleys, while larger R_{sk} values are typical of profiles with isolated, steep peaks. Smoother surfaces will have smaller R_{ku} values, while surfaces with steep asperities will exhibit larger R_{ku} values. Figure 8 shows a schematic of surfaces with varying R_{sk} and R_{ku} values. As the R_{sk} becomes smaller, the asperities on the rough surface develop large plateaus with single deep valleys, and as the R_{ku} becomes smaller, the surface becomes smoother (Ref 20). Contact with a surface having smaller R_{sk} and R_{ku} values will be improved as the asperities become flatter and smoother (Fig. 8).

Experiments have shown that when the cooling rates are higher, more of the splat remains on the Inconel surface, suggesting that the splat-substrate adhesion has improved. It has been shown that, for solid surfaces with similar R_a, the adhesion characteristics may vary significantly and may depend on the magnitudes of R_{sk} and R_{ku} (Ref 21). Larger R_{sk} and R_{ku} values reduce the real area of contact between two surfaces, reducing the adhesion between the surfaces (Ref 20). Table 2 shows the results of the R_a, R_{sk}, and R_{ku} for nonheated and preheated Inconel. Preheating the Inconel substrates increases the R_a, while decreasing R_{sk} and R_{ku}. The increase in R_a provides more asperities for contact with the liquid splat (Ref 10, 12), while the decrease in R_{sk} and R_{ku} increases the area of contact between the splat and the asperities, promoting splat adhesion to the preheated Inconel. The average final diameter of the splat on preheated Inconel was 15% larger than on nonheated Inconel, resulting in a 30% increase in the final area of the splat that remained on the surface. The increase in the splat cooling rate on the preheated surface may also be attributed to changes in the

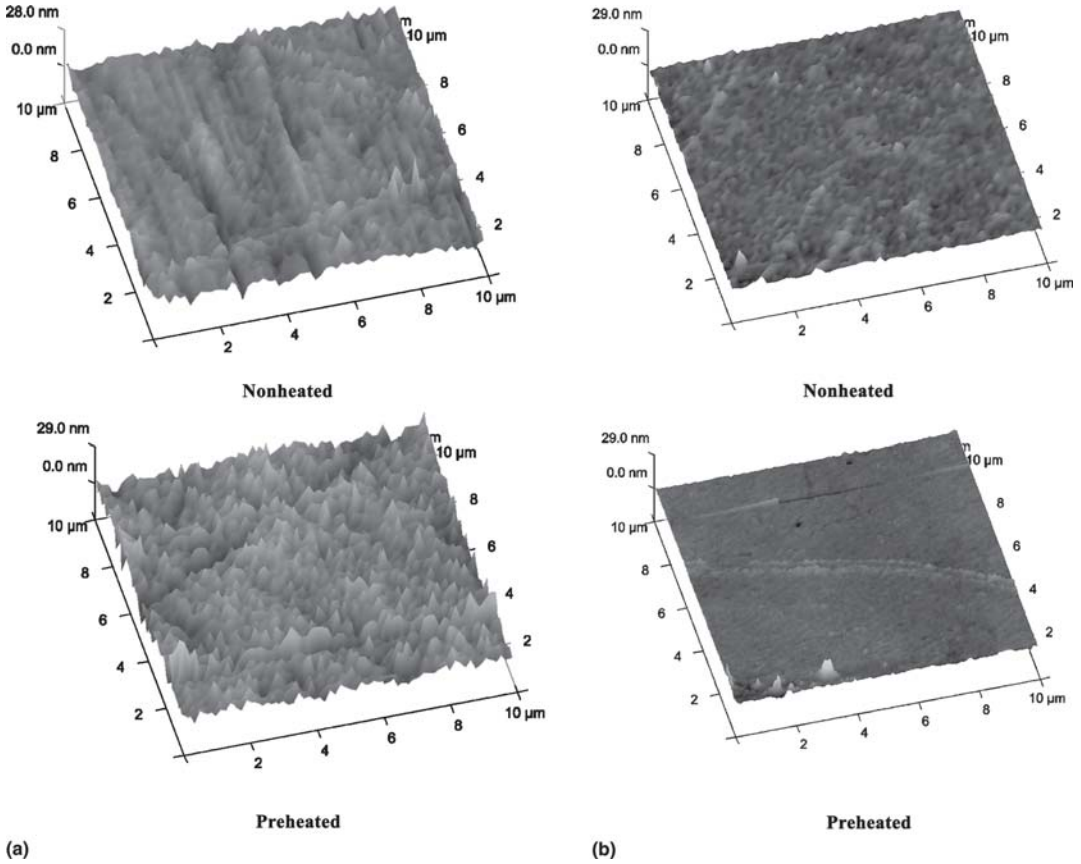

Fig. 7 Surface topologies of (a) Inconel and (b) glass before (top) and after (bottom) prolonged preheating at 400 °C

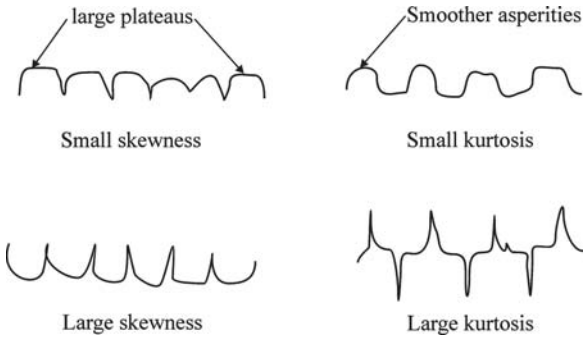

Fig. 8 Schematic of surfaces with varying R_{sk} and R_{ku} values

surface topology. With lower R_{sk} and R_{ku} values and increased splat contact with the asperities on the preheated surface, the transfer of heat from the splat to the substrate was increased. Cedelle et al. (Ref 12) have also observed an increase in the splat cooling rates on preheated stainless steel surfaces.

The increased contact and cooling rate of the splats on preheated Inconel will increase the viscosity of the liquid. This will increase the losses due to viscous dissipation in the spreading splat, reducing the initial energy and resulting in smaller maximum spread diameters (Ref 22). On preheated Inconel, where the splat contact is improved and cooling rates are increased (Table 1) due to lower R_{sk} and R_{ku} values (Table 2), the maximum spread diameters were ~30% lower than those on nonheated Inconel.

Table 2 Average roughness, skewness, and kurtosis of Inconel substrates

Inconel 625	R_a, nm	R_{sk}	R_{ku}
Nonheated	2.0	0.20	7.0
Preheated	3.5	−0.01	6.0

It has been shown in this study that preheating glass does not affect the surface topology significantly (Fig. 7b). Figure 9 shows the thermal emissions of molybdenum droplets impinging on both heated and unheated surfaces (Fig. 9a), photographs of the splats on both surfaces (Fig. 9b), and SEM images of the splats left adhering to the substrates after impact (Fig. 9c). Thermal emission signals and images of molybdenum splats at the maximum extent on nonheated and preheated glass were similar. The average maximum spread diameter on both substrates was 410 ± 10 µm. The maximum spread time on preheated glass was 1.8 ± 0.2 µs, ~12% larger than that on nonheated glass (1.6 µs). Figure 9(a) confirms that the maximum spread diameters on the samples of nonheated and preheated glass were approximately equal, because the maximum voltages of their thermal emission signals were almost the same. Material loss also occurs within 3 µs after impact on both surfaces. Typical final, solidified cores of the splat remaining after solidification and the material loss on

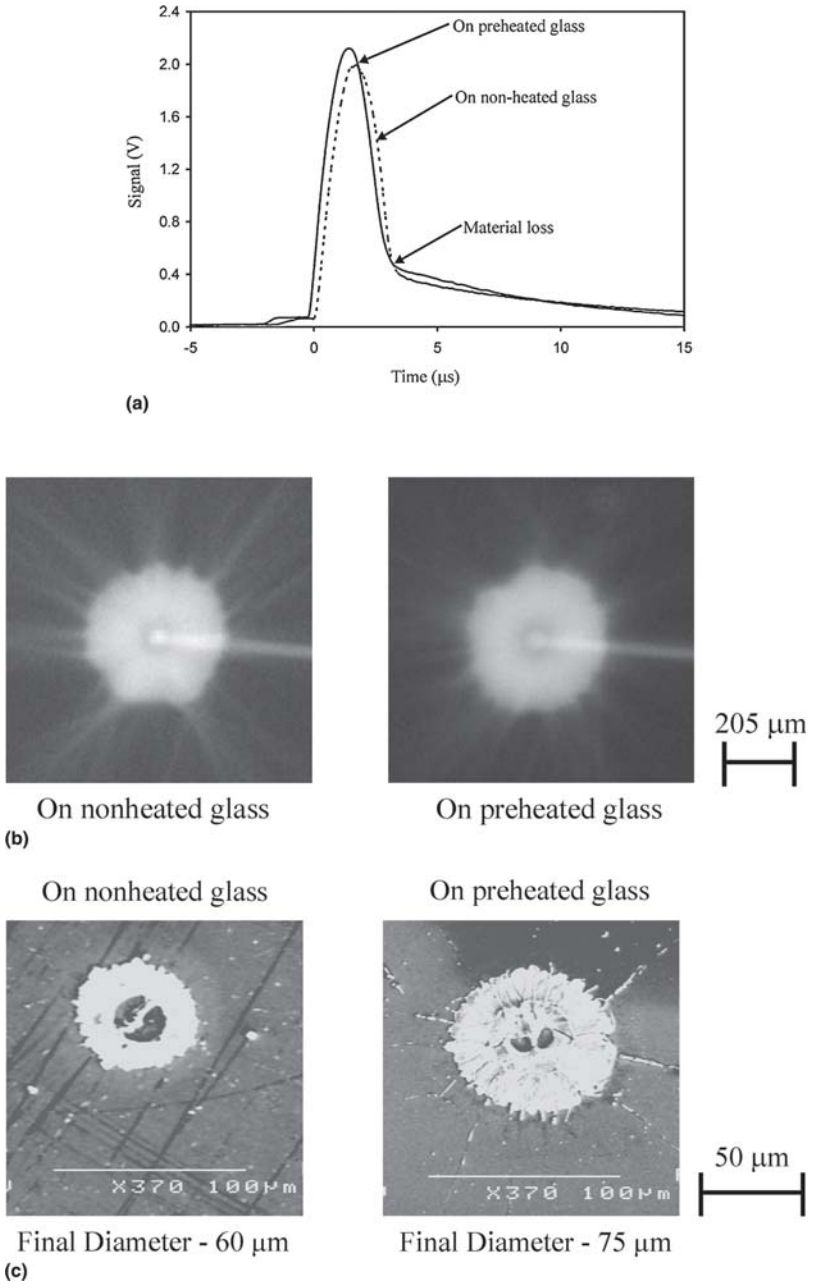

Fig. 9 (a) Thermal emission signals, (b) images of splats at the maximum extent on nonheated and preheated glass, and (c) images after solidification

the two glass surfaces are shown in Fig. 9(c). The similarities that exist between splats on nonheated and preheated glass suggest that preheating glass does not affect significantly the splat morphology, maximum diameter, and the occurrence of fragmentation and material loss.

4. Conclusions

The influence of substrate temperature and surface topology on the morphology, the maximum spread diameter, and the cooling rate of plasma-sprayed molybdenum particles on a metal surface was studied. Plasma-sprayed molybdenum particles that impacted Inconel maintained at room temperature had a maximum spread diameter that was almost three times that on Inconel maintained at 400 °C. The cooling rate, as calculated from two-color pyrometric signals, was more than three times larger on the heated Inconel, suggesting that thermal contact was improved.

Particles impacting Inconel that was preheated for 3 h at 400 °C and then cooled, had splat maximum diameters that were smaller and cooling rates that were two times larger than those on nonheated Inconel. This was attributed to the increased R_a and the decreased R_{sk} and R_{ku} of the preheated metal. The roughness parameters and surface topology changed due to the growth

of an oxide layer. The oxide layer improved the contact between the splat and the surface, which increased the splat cooling rate and decreased the maximum spread diameter. Significant changes in the splat morphology, the occurrence of material loss, and the splat maximum diameter were not observed when glass was preheated.

Acknowledgment

This work was funded by the Natural Sciences and Engineering Research Council of Canada (NSERC).

References

1. M. Fukumoto, E. Nishioka, and T. Matsubara, Flattening and Solidification Behavior of a Metal Droplet on a Flat Substrate Surface Held at Various Temperatures, *Surf. Coat. Technol.,* 1999, **120-121,** p 131–137
2. C. Moreau, J. Bisson, R. Lima, and B. Marple, Diagnostics for Advanced Materials Processing by Plasma Spraying, *Pure Appl. Chem.,* 2005, **77**(2), p 443-462
3. N. Mehdizadeh, M. Lamontagne, C. Moreau, S. Chandra, and J. Mostaghimi, Photographing Impact of Molten Molybdenum Particles in a Plasma Spray, *J. Thermal Spray Technol.,* 2005, **14,** p 354-361
4. S. Costil, H. Liao, A. Gammoudi, and C. Coddet, Influence of Surface Laser Cleaning Combined With Substrate Preheating on the Splat Morphology, *J. Thermal Spray Technol.,* 2005, **14**(1), p 31-38
5. J. Pech, B. Hannoyer, L. Bianchi, P. Fauchais, and A. Denoirjean, Study of Oxide Layers Obtained Onto 304L Substrates Heated by a DC Plasma Jet, *Thermal Spray: A United Forum for Scientific and Technological Advances,* C.C. Berndt, Ed., September 15-18, 1997 (Indianapolis, IN), ASM International, 1998, p 775–782
6. C. Li, J. Li, and W. Wang, The Effect of Substrate Preheating and Surface Organic Covering on Splat Formation, *Thermal Spray: Meeting the Challenges of the 21st Century,* C. Coddet, Ed., May 25-29, 1998 (Nice, France), ASM International, 1998, p 473–480
7. X. Jiang, Y. Wan, H. Hermann, and S. Sampath, Role of Condensates and Adsorbates on Substrate Surface on Fragmentation of Impinging Molten Droplets During Thermal Spray, *Thin Solid Films,* 2001, **385,** p 132-141
8. A. McDonald, M. Lamontagne, C. Moreau, and S. Chandra, Visualization of Impact of Plasma-Sprayed Molybdenum Particles on Hot and Cold Glass Substrates, *International Thermal Spray Conference 2005, Plasma Spraying,* E. Lugscheider, Ed., May 2-4, 2005 (Basel, Switzerland), ASM International, 2005, p 1192–1197
9. V. Pershin, M. Lufitha, S. Chandra, and J. Mostaghimi, Effect of Substrate Temperature on Adhesion Strength of Plasma-Sprayed Nickel Coatings, *J. Thermal Spray Technol.,* 2003, **12,** p 370-376
10. M. Fukumoto, I. Ohgitani, M. Shiiba, and T. Yasui, Effect of Substrate Surface Change by Heating on Transition in Flattening Behavior of Thermal Sprayed Particles, *Thermal Spray 2004: Advances in Technology and Application, Characterization Methods for Coating Properties (V),* E. Lugscheider and C.C. Berndt, Ed., May 10-12, 2004 (Osaka, Japan), ASM International, 2004, p 1-6
11. P. Chauvy, C. Madore, and D. Landolt, Variable Length Scale Analysis of Surface Topography: Characterization of Titanium Surfaces for Biomedical Applications, *Surf. Coat. Technol.,* 1998, **110,** p 48-56
12. J. Cedelle, M. Vardelle, B. Pateyron, P. Fauchais, M. Fukumoto, and I. Ohgitani, Plasma-Sprayed Particles: Impact Imaging and Flattening Particle Thermal History, *International Thermal Spray Conference 2005, Process Diagnostics (I),* E. Lugscheider, Ed., May 2-4, 2005 (Basel, Switzerland), ASM International, 2005, p 656–661
13. K. Shinoda, Y. Kojima, and T. Yoshida, In Situ Measurement System for Deformation and Solidification Phenomena of Yttria-Stabilized Zirconia Droplets Impinging on Quartz Glass Substrate Under Plasma-Spraying Conditions, *J. Thermal Spray Technol.,* 2005, **14**(4), p 511-517
14. M. Vardelle, A. Vardelle, A. Leger, P. Fauchais, and D. Gobin, Influence of Particle Parameters at Impact on Splat Formation and Solidification in Plasma Spraying Processes, *J. Thermal Spray Technol.,* 1994, **4**(1), p 50-58
15. C. Moreau, P. Cielo, M. Lamontagne, S. Dallaire, and M. Vardelle, Impacting Particle Temperature Monitoring During Plasma Spray Deposition, *Meas. Sci. Technol.,* 1990, **1,** p 807-814
16. P. Gougeon and C. Moreau, Simultaneous Independent Measurement of Splat Diameter and Cooling Time During Impact on a Substrate of Plasma-Sprayed Molybdenum Particles, *J. Thermal Spray Technol.,* 2001, **10,** p 76-82
17. J.R. Taylor, *An Introduction to Error Analysis: The Study of Uncertainties in Physical Measurements,* University Science Books, Mill Valley, CA, 1982, p 89
18. C. Moreau, P. Gougeon, and M. Lamontagne, Influence of Substrate Preparation on the Flattening and Cooling of Plasma-Sprayed Particles, *J. Thermal Spray Technol.,* 1995, **4**(1), p 25-33
19. L. Li, X. Wang, G. Wei, A. Vaidya, H. Zhang, and S. Sampath, Substrate Melting During Thermal Spray Splat Quenching, *Thin Solid Films,* 2004, **468,** p 113-119
20. N. Tayebi and A. Polycarpou, Modeling the Effect of Skewness and Kurtosis on the Static Friction Coefficient of Rough Surfaces, *Tribology Int.,* 2004, **37,** p 491-505
21. R. Alley, K. Komvopoulos, and R. Howe, Self-Assembled Monolayer Film for Enhanced Imaging of Rough Surfaces With Atomic Force Microscopy, *J. Appl. Phys.,* 1994, **76,** p 5731-5737
22. M. Pasandideh-Fard, V. Pershin, S. Chandra, and J. Mostaghimi, Splat Shapes in a Thermal Spray Coating Process: Simulations and Experiments, *J. Thermal Spray Technol.,* 2002, **11,** p 206-217